THERMAL RESPONSE OF THERMOPLASTIC COMPOSITE TAPE DURING IN-SITU CONSOLIDATION AUTOMATED FIBER PLACEMENT USING A LASER HEAT SOURCE

Tyler B. Hudson[1], Charles T. Dolph[2], Garrett M. Grose[2], Roberto J. Cano[1], Ryan F. Jordan[3], Christopher J. Wohl[1], Rodolfo I. Ledesma[4], Brian W. Grimsley[1]

[1]NASA Langley Research Center, Hampton, VA 23681
[2]NASA Internships, Fellowships, and Scholarships (NIFS), NASA Langley Research Center, Hampton, VA 23681
[3]Electroimpact, Inc., Mukilteo, WA 98175
[4]National Institute of Aerospace (NIA), Hampton, VA 23666

ABSTRACT

Composite materials have tremendous potential in the design and manufacture of commercial aircraft due to their high strength-to-weight and stiffness-to-weight properties. However, the use of composite materials is currently limited by high cost and long manufacturing time. The National Aeronautics and Space Administration (NASA) initiated the Hi-rate Composite Aircraft Manufacturing (HiCAM) project to investigate promising composite processing technologies with a goal of vastly improving composite commercial aircraft manufacturing rate (4 to 6 times faster than current production rates). Laser assisted automated fiber placement (AFP) of thermoplastics is a key technology that could increase speed of composite manufacturing, but the technology has not been fully developed. In-situ consolidation AFP of thermoplastics (ICAT) could reduce time and cost even further by eliminating the time and equipment required for post-consolidation. In this work, the thermal response of laser heated ICAT was investigated using forward looking infrared (FLIR) and embedded thermocouples (TCs) to better understand fusion between layers (autohesion). Detailed explanation of the algorithm to combine FLIR and TC data will be presented. In addition, the effect of robot speed on time above melting temperature was quantified.

Keywords: Laser Heating, Automated Fiber Placement (AFP), In-situ Consolidation, Polyetherketoneketone, Thermoplastic Composites

Corresponding author: tyler.b.hudson@nasa.gov

1. INTRODUCTION

Aircraft manufacturing is a cornerstone of the United States economy. Commercial aircraft were the largest single category of export from the United States in 2019 [1]. Worldwide, the market for

single-aisle aircraft is projected to grow by \$36.9 billion from 2021 (\$85.7 billion) to 2027 (\$122.6 billion), making production of this type of aircraft crucial to the United States economy [2].

Composites have tremendous potential in airframe construction. They are attractive to aircraft manufacturers and designers because of their favorable mechanical properties and resistance to corrosion [3]. These properties enable the construction of aircraft that are significantly lighter, and therefore more fuel efficient. This will both lower the cost of air travel and improve environmental outcomes.

Small aircraft have long incorporated composite materials, but commercial transport aircraft made with composites have only entered production relatively recently [6]. Passenger aircraft with a large proportion of their airframe constructed using carbon fiber reinforced composites are currently being manufactured, but composites are considered harder to manufacture and more costly compared to metallic airframes [5]. New manufacturing technologies and processes are vital to ensure that production of next generation aircraft can keep up with demand.

In 2021, the Hi-rate Composite Aircraft Manufacturing (HiCAM) project was initiated by the National Aeronautics and Space Administration (NASA) to investigate technologies for rapid production of commercial airframes using composite materials. HiCAM aims to advance multiple technologies to technology readiness level (TRL) 6-7 by the year 2027. One area being investigated is automated fiber placement (AFP) of thermoplastics. During this process, polyaryletherketone thermoplastic prepreg (pre-impregnated carbon fiber) tape is placed robotically (Figure 1, Figure 2). The current state-of-art (SoA) AFP process uses thermoset prepreg tapes, which must be cured in an autoclave after placement. Switching to a thermoplastic matrix could eliminate the need for autoclave curing.

In-situ consolidation AFP of thermoplastics (ICAT) presents many engineering challenges, which have yet to be solved [8]. Maximizing the speed the robot applies composite tape (layup speed) is critical to making the process economically viable. Effective consolidation also requires large amounts of thermal energy because of the higher melting temperature of polyaryletherketones, semi-crystalline thermoplastic materials. Therefore, lasers are a popular heating solution for their high-power output, ability to tightly focus the heating zone, and uniform power distribution [9, 10, 11]. Understanding the thermal behavior of the composite materials during laydown using laser heating is crucial to assessing its viability. To this end, the temperature history of the matrix material during layup must be quantified. Some studies have used embedded thermocouples (TCs) to monitor temperature in the ply below active layup [12, 13]. TCs in this location are insulated by a layer of prepreg material, so this information does not reflect the thermal response of the surfaces that are actively being melted and fused, where the highest temperatures occur.

Within this work, three panels were fabricated using laser-assisted ICAT and varied process parameters. Temperature was monitored at different locations throughout each panel to give insight into the thermal response of the thermoplastic matrix and temperature history at individual points. A measurement artifact similar to that reported by Stokes-Griffin et al. [14] was observed, and a mathematical method was developed to correct for this artifact.

2. EXPERIMENTATION

2.1 Equipment

Fabrication was performed at Electroimpact Inc. in Mukilteo, WA, USA with a six-axis Kuka Titan® robotic arm with an Electroimpact developed QS16 placement head. The AFP head was configured to place 2.54-cm wide courses comprised of four 0.635-cm wide carbon fiber/thermoplastic matrix tapes (Figure 1) onto a custom, 9.5-mm thick, aluminum tool that was heated by a uniform hotplate supplied by Wenesco®. Electroimpact 400 W per lane, 976-nm wavelength, VSSL-HP (Variable Spot Size Laser-High Power) was mounted to the AFP head and used to heat both the incoming and substrate tape, simultaneously. The laser used four rectangular spots (one for each tape), which could be controlled individually. A conformable compaction roller was used to apply force to the incoming and substrate heated tapes. Panels were placed on a layer of high-temperature polyimide release film (DuPont™ Kapton®) attached to the heated tool to prevent sticking. A schematic diagram of the layup process can be seen in Figure 2, where the angle of incidence (θ) is approximately 16 degrees.

Figure 1: Electroimpact six-axis AFP robot arm (Image Credit: Electroimpact, Inc.).

Temperature was measured during layup with two separate systems. A forward-looking infrared (FLIR) camera supplied by Teledyne FLIR® was mounted to the AFP head. This camera monitored the temperature distribution on the incoming tape and the substrate during the layup process. Calibration of the FLIR camera was achieved by pointing it directly down at a layer of prepreg material on the heated tool and determining the correct emissivity value to match temperatures measured by surface mounted TCs. Further improvements/validation of the FLIR emissivity calibration process are needed since the calibration was performed at lower temperatures than those observed by the FLIR camera during processing. The emissivity value of the FLIR was found to be 0.8 for the composite material.

J-type, 40 AWG, TCs (5TC-TT-J-40-36 from Omega®) were also used to monitor substrate temperature throughout layup. TCs were "welded" onto the surface of the substrate tape by melting the surface polymer using a hand-held soldering iron. "Welding" the TCs prevented them from moving during layup and minimized protrusion of the TC bead from the substrate surface. A DATAQ® DI-2008 data acquisition (DAQ) system was used to collect temperature data at a rate of 2 kHz, which made it possible to observe the evolution of the substrate temperature over a very short time period (~1.5 s) with relatively high fidelity.
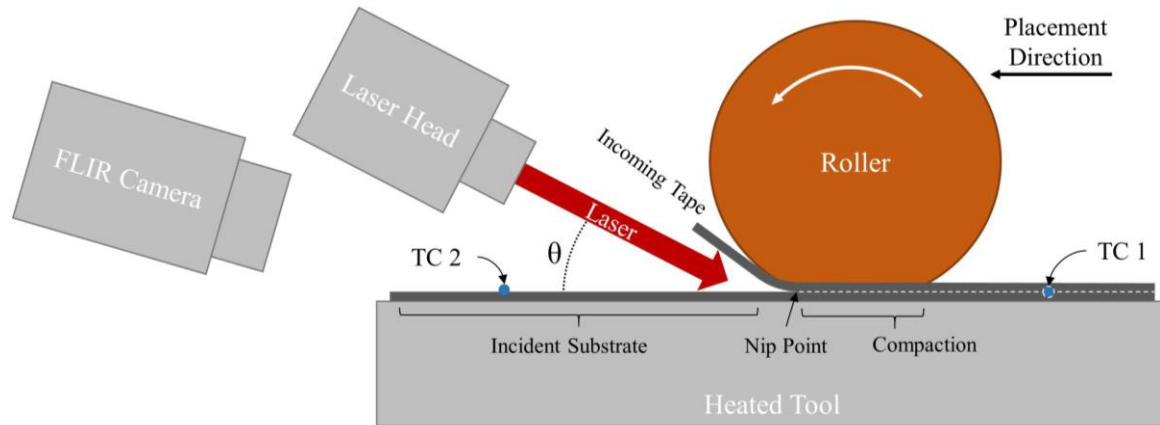

Figure 2: Schematic diagram of laser-assisted AFP.

2.2 Materials and Experiment Design

An IM7 carbon fiber/polyetherketoneketone (PEKK) thermoplastic tape was supplied by Hexcel® with an areal weight of 194 gsm, 34wt.% resin content, and thermal properties shown in Table 1 was used in this study. Four tows, each 6.35-mm (0.25-in.) wide, were applied simultaneously by the AFP robot.

Table 1: Slit tape material thermal properties.

Slit-tape Material:	Melt Temperature (T_m)*	2% Mass Loss Decomposition Temperature**	Glass Transition Temperature (T_g)*
Hexcel IM7/PEKK	340°C	546°C	160°C

*Measured using differential scanning calorimetry (DSC) on as-received Hexcel IM7/PEKK tape from the same batch as the ICAT processing experiments.

**Measured using thermal gravimetric analysis (TGA) on as-received Hexcel IM7/PEKK tape.

Three, 50.8 cm × 25.4 cm (20 in. × 10 in.), composite panels with 24-ply, quasi-isotropic layups, [45/0/-45/90]$_{3S}$, were fabricated with the processing parameters shown in Table 2. The primary objective was to understand thermal response with a wide range of layup speeds. The laser power used for each panel was empirically determined to produce the desired target surface temperature of the prepreg tape as measured by the FLIR camera for each layup speed. The peak temperature was selected to balance maximizing time above melt (higher temperatures preferred) while minimizing/preventing decomposition (lower temperatures preferred). The first ply of all three panels was placed with a layup speed of 150 mm/s and laser power of 85 W based on previous placement studies, demonstrating these parameters ensured adherence of the prepreg tape to the Kapton® film. Therefore, the values for layup speed and average laser power in Table 2 only describe plies two through twenty-four.

Table 2: Panel fabrication parameters.

Panel	Layup Speed (mm/s)	Average Laser Power (W)	Tool Temperature (°C)	Target Peak Surface Temperature (°C)
A	25	61	180	525
B	50	89	180	525
C	100	133	200	550

Pairs of TCs were placed after plies 1, 14, and 22 (Figure 3). Thus, TC temperature measurements are recorded during the layup of plies 2, 15, and 23 (all zero-degree plies), respectively. This placement of TCs allowed for comparison of thermal response at a variety of locations throughout the panel.

Figure 3: TC numbers and locations.

2.3 Scaling TC Data Based on FLIR Measurements

The FLIR camera provides the temperature of the substrate and incoming tape up to the nip point. In this work, the nip point is defined as first contact of the substrate with the incoming tape (Figure 2). The TCs provide temperature measurements from prior to and underneath the roller as well as at the ply interface during cooldown, as the heating/compaction zone moves along its programmed path. However, the raw TC measurements were not representative of the actual temperature of the substrate material during laser heating and for the initial portion of cooldown. The majority of the TCs recorded a temperature that was significantly higher than the average temperature recorded by the FLIR camera, in some cases by several hundred degrees Celsius. It was determined that the TCs were not measuring the actual temperature of the surrounding thermoplastic tape material during laser heating and initial cooldown because the TC readings were higher than the material decomposition temperature, and no damage was observed in the tape material. It was assumed that the TC reading was a true indication of the TC temperature, not an error in performance. One possibility for the TC temperature exceeding the surrounding material is that the materials used in the construction of the thermocouple (iron and constantan) are more absorptive of the laser light, causing them to heat faster than the substrate. In addition, despite efforts to "weld" the TCs into the substrate (Figure 4) using a soldering iron, the TCs sit proud of the substrate surface. Because the TC sits proud, the angle of incidence on the TC was higher, and more inconsistent, than the angle of incidence on the substrate (Figure 5), which results in higher intensity on the surface of the TC.
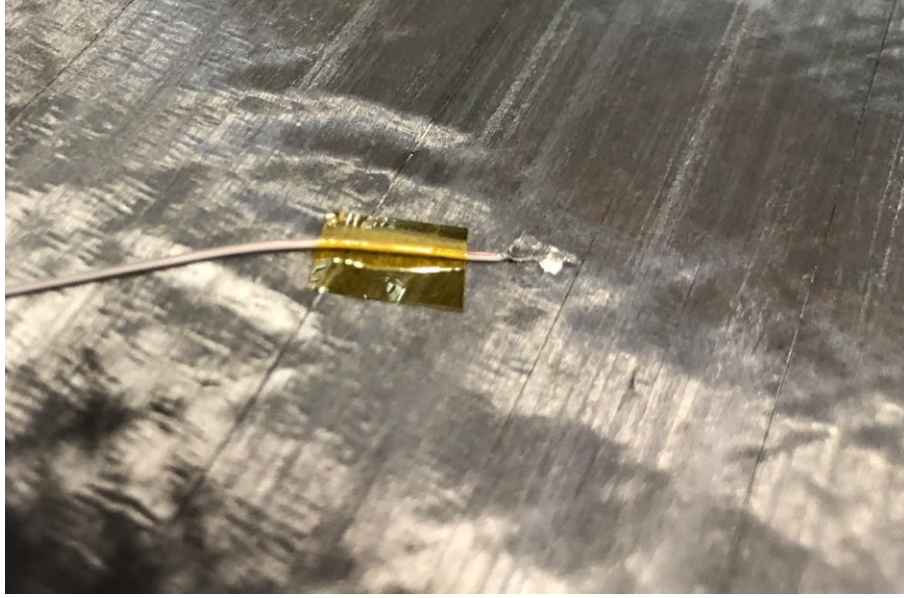
Figure 4. Photograph of TC following "welding" into thermoplastic composite surface using flat tip soldering iron (Image Credit: NASA).
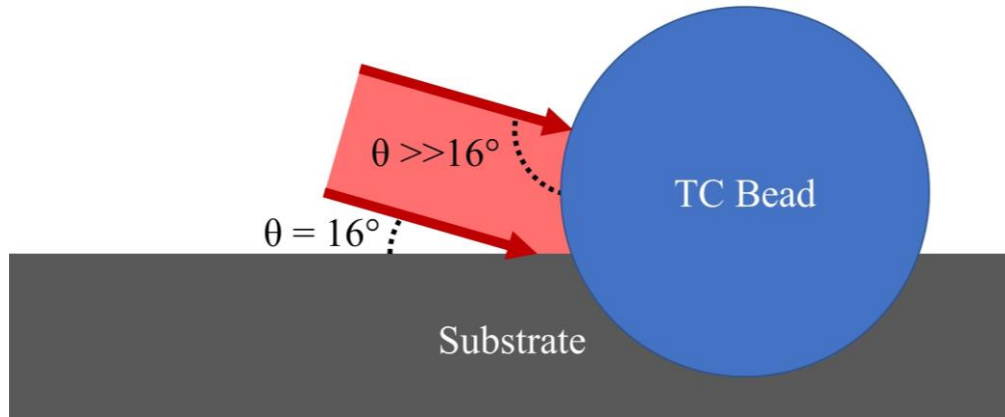

Figure 5: Angle of incidence diagram.

For this work, the peak temperature of the composite material was measured by the FLIR camera and was used to scale TC data to depict substrate temperature during laser heating and cooldown. More work is needed in this area to confirm/validate the peak temperature at the nip point. The scaled TC curve is calculated using equations (1) and (2).

$$T_{base} = T_{raw}\left(t_{offset(heating,cooldown)}\right) \qquad (1)$$

$$T_{scaled}(t) = T_{base} + \frac{T_{raw}(t) - T_{base}}{T_{max} - T_{base}} \cdot (T_{FLIR} - T_{base}) \qquad (2)$$

$T_{raw}(t)$	=	Unscaled TC temperature as a function of time.
$t_{offset(heating)}$	=	-0.5 s (heating regime).
$t_{offset(cooldown)}$	=	2 s (cooling regime).
T_{base}	=	TC temperature at t_{offset}.
T_{FLIR}	=	Maximum FLIR temperature of the tow above the TC (assumed to be nip point temperature).
T_{max}	=	Maximum recorded TC temperature.
$T_{scaled}(t)$	=	Scaled TC temperature as a function of time.

3. RESULTS AND DISCUSSION

3.1 Scaling TC Data Based on FLIR Measurements

Maximum FLIR temperature (T_{FLIR}) is the temperature at the center of the tow that covered the TC averaged over the entire course. In this work, this value is assumed to be the nip point temperature. $T_{scaled}(t)$ was calculated separately for the heating regime and the cooling regime and combined during post-processing. The only difference between the calculation for the heating and cooling regime is the value of t_{offset}, which was chosen to correspond with a value of $T_{raw}(t)$ that was unaffected by the laser heating of the TC (i.e., where the temperature of the TC was assumed to match the surrounding composite material). The method of scaling the TC data based on the peak temperature measured by the FLIR camera is visually depicted in Figure 6.
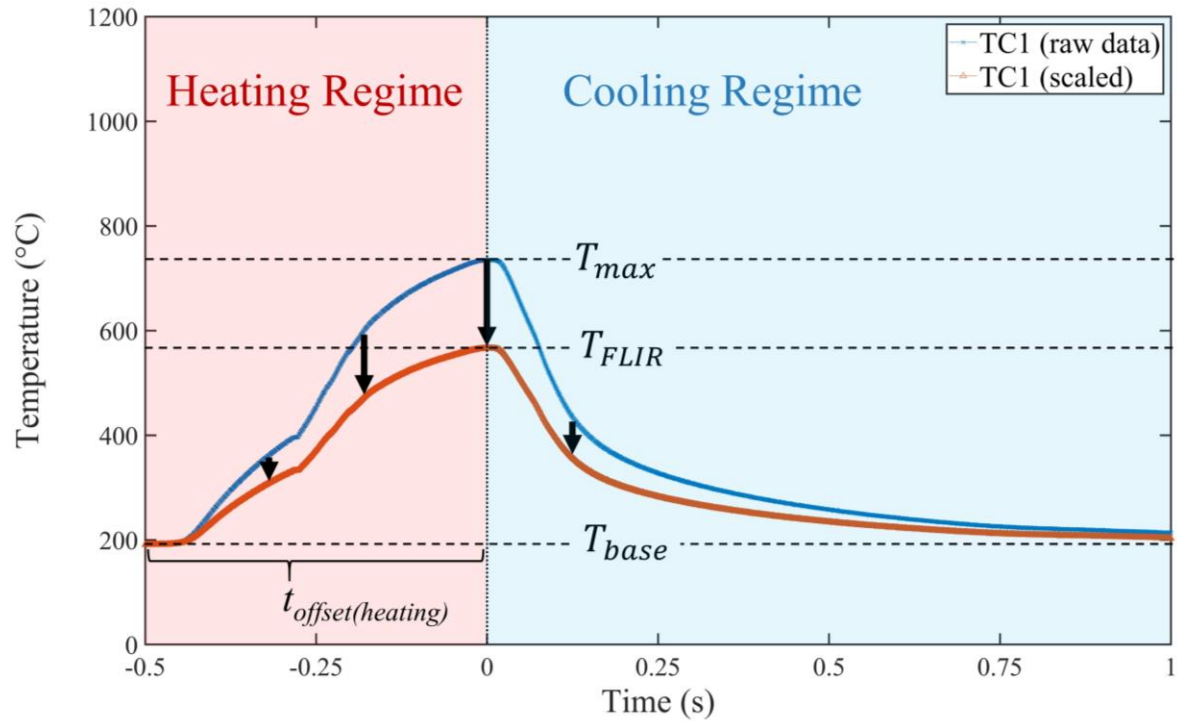

Figure 6: TC scaling visualization for Panel A: TC1.

3.2 Effect of Heated Tool on Cooling Regime

During cooling, it was observed that TC1 and TC2 approached the heated tool temperature quicker than TCs 3-6. TCs 1 and 2 were only separated from the heated tool by one sheet of Kapton® and one ply of composite, as compared to 14 plies for TC3 and TC4 and 22 plies for TC5 and TC6. The additional composite plies insulate the joining interface from the aluminum heated tool. This phenomena is especially visible in the tail of the cooldown curve (0.25 s to 1 s in Figure 7).
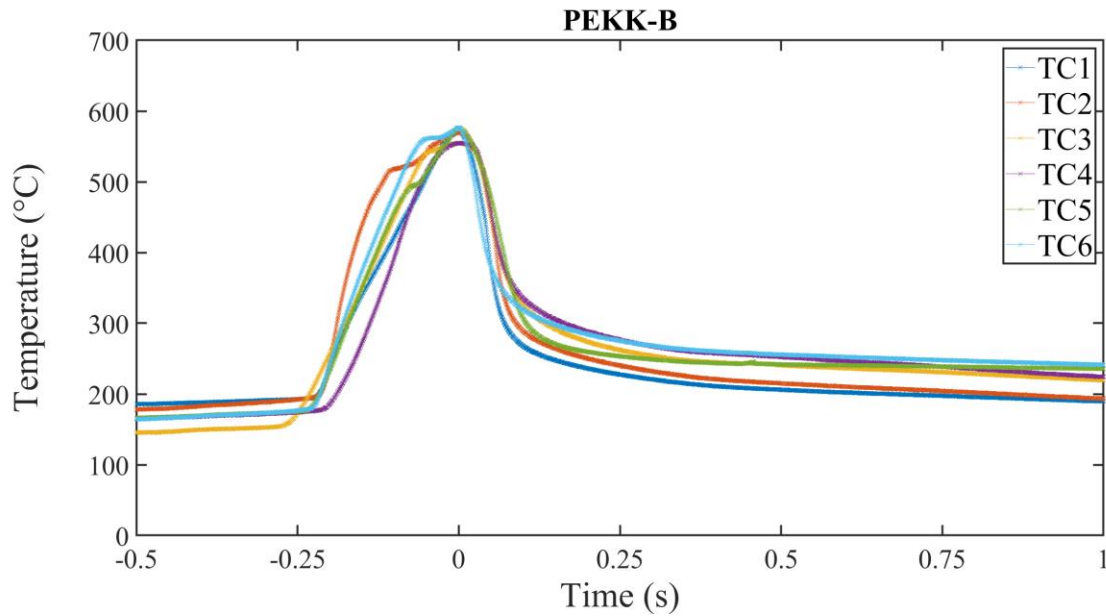

Figure 7: Scaled temperature data from all six TCs for Panel B [Layup Speed: 50 mm/s, Tool Temperature: 180°C, Target Peak Surface Temperature: 525°C].

3.3 Time Above Melt Temperature

Temperature curves from the same TC location in each panel were plotted to compare the shape of each curve as well as the relative time each location spent above the material melt temperature ($T_m = 340°C$, Table 1). The plot for TC3 is shown in Figure 8, which is a good representation of the data set as a whole.
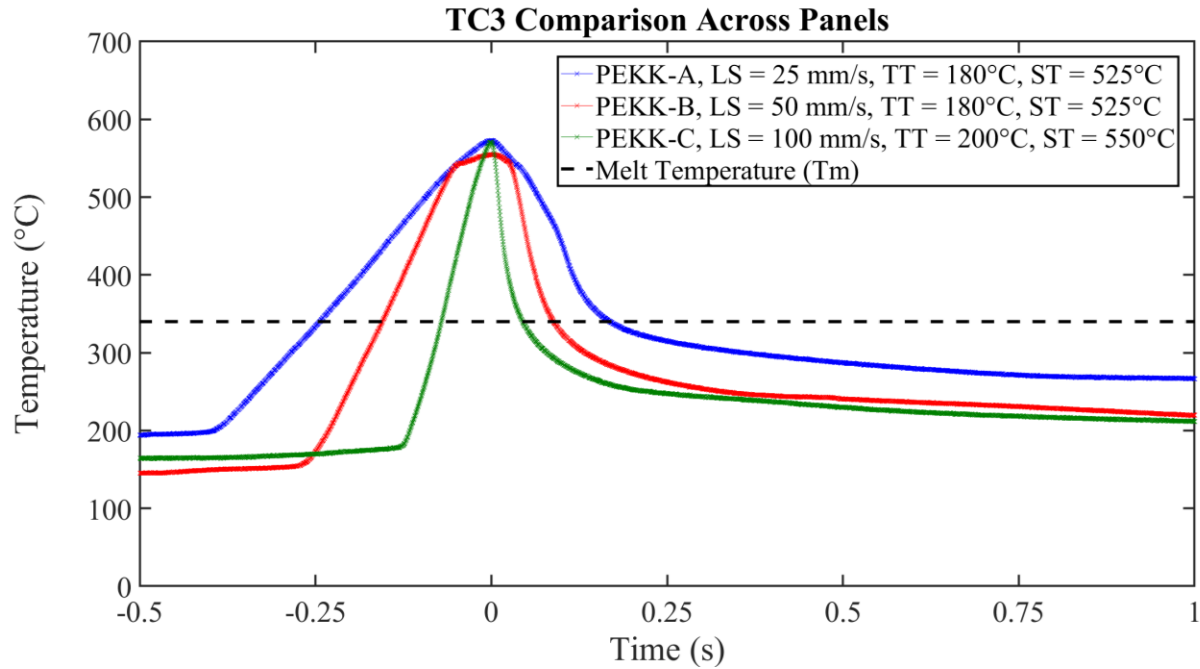
Figure 8: Comparison of times above melt temperature at TC3 for panels A, B, and C [Legend key: Layup Speed (LS), Tool Temperature (TT), and Target Peak Surface Temperature (ST)].

Peak temperatures were similar across all panels, with an average of 574°C and a standard deviation of 12°C, which indicates that the values chosen for the laser power at each ply effectively produced similar maximum temperatures despite significantly different layup speeds. The peak temperatures shown in Figure 8 are significantly higher than the target surface temperature because they are taken from the center of a laser spot. In contrast, the target surface temperature represents an average across all four tows in the course. Slower placement speed led to longer time above melt temperature in all cases. Slower speed and lower laser power allow for more thermal energy to be absorbed into the composite material prior to reaching the desired target surface temperature. To better understand this phenomenon, average time above melt temperature was calculated in multiple ways. The average total time above melt temperature for all TCs is shown in Figure 9a. TC1 and TC2 are omitted from Figure 9b to remove the tool effect from the data. The average time above melt temperature after the peak temperature is reached with and without the tool effect is shown Figure 9c and Figure 9d, respectively. The best representation of the cooldown behavior throughout the composite is shown in Figure 9d. The results shown in Figure 9d indicate there was a statistically significant longer time above melting temperature for panel A, while panels B and C are within error bars (one standard deviation). The variability in the time above melt during cooldown was higher for panel C than panels A and B.
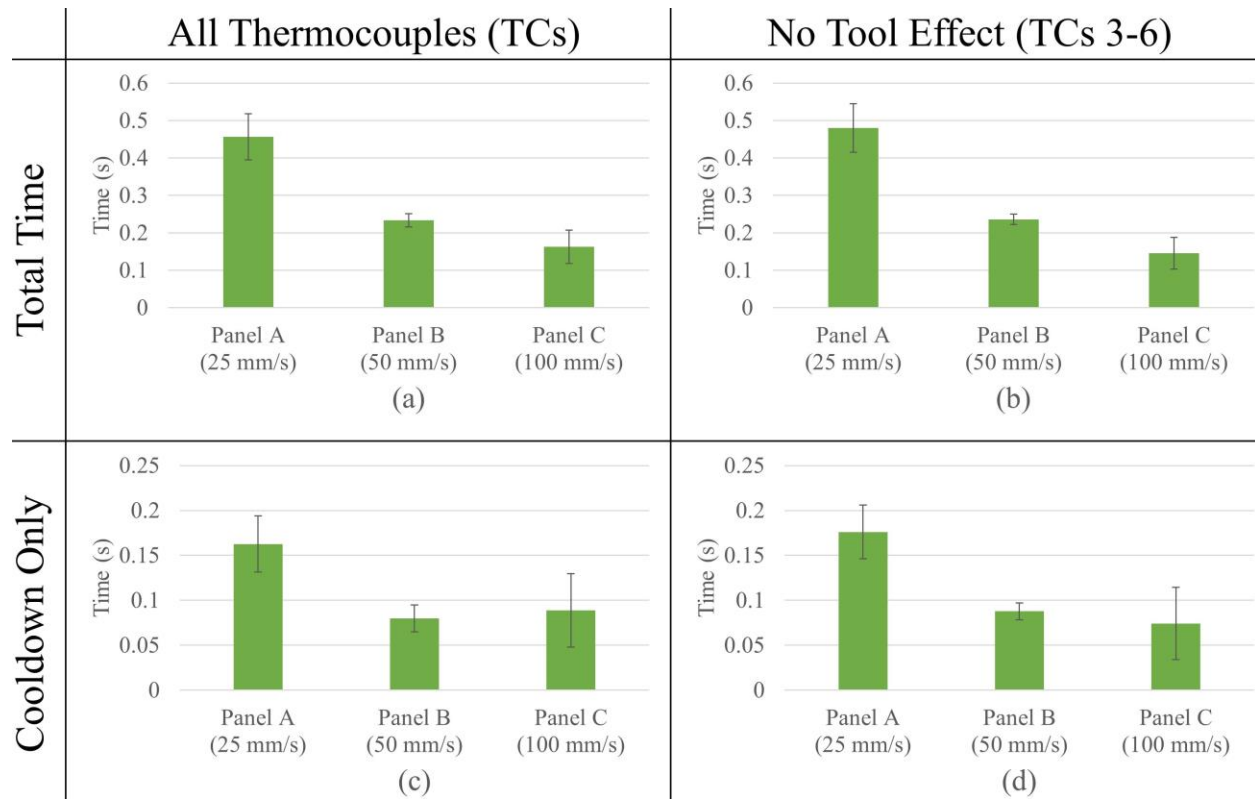
Figure 9: Average time above melt temperature comparison matrix. Error bars indicate one standard deviation [$n = 6$ for (a) and (c) and $n = 4$ for (b) and (d)].

4. SUMMARY

Composite panels with a semi-crystalline thermoplastic matrix (IM7/PEKK) were fabricated using a laser-assisted AFP process. Three layup speeds were chosen to be investigated in this study. Temperature data was collected by a FLIR camera and a TC data acquisition system. Peak temperature was determined using the FLIR camera and combined with the TC data to enable a complete time history of the joining interface to be determined. The time above melt temperature for each layup speed was compared and slower placement speeds were observed to increase time above melt temperature.

Future work will include post-processing of these panels. Each panel will be cut into three segments. One segment will not be post-consolidated (ICAT only). One segment will be consolidated using a pressurized autoclave and vacuum bag and another using an oven with vacuum bag only (VBO) pressure. Ultrasonic scanning and mechanical testing will be performed to relate layup speed and post-processing to porosity and mechanical properties.

5. REFERENCES

[1] C. P. Kimberly Amadeo, "US Exports: Top Categories, Challenges, and Opportunities," The Balance, 4 March 2021. [Online]. Available: https://www.thebalancemoney.com/u-s-exports-top-categories-challenges-opportunities-3306282. [Accessed 6 December 2022].

[2] "Single-Aisle Aircraft Market," Virtue Market Research, August 2022. [Online]. Available: https://virtuemarketresearch.com/report/single-aisle-aircraft-market/description. [Accessed 6 December 2022].

[3] R. Boyer, J. Cotton, M. Mohaghegh and R. Schafrik, "Materials considerations for aerospace applications," *MRS Bulletin,* vol. 40, no. 12, pp. 1055-1066, 2015. doi:10.1557/mrs.2015.278.

[4] "Boeing's Dreamliner completes first commercial flight," 6 October 2011. [Online]. Available: https://www.bbc.com/news/business-15456914. [Accessed 6 December 2022].

[5] L. Zhu, N. Li and P. Childs, "Light-weighting in aerospace component and system design," *Propulsion and Power Research,* vol. 7, no. 2, pp. 103-119, 2018. https://doi.org/10.1016/j.jppr.2018.04.001.

[6] B. W. Grimsley, R. J. Cano, T. B. Hudson, F. L. Palmieri, C. J. Wohl, T. Sreekantamurthy, C. J. Stelter, M. A. Assadi, R. F. Jordan, R. A. Edahl, J. C. Shiflett, J. C. Connell and B. J. Jensen, "High-rate aircraft manufacturing: In-situ consolidation AFP of thermoplastic composites for high-rate aircraft manufacturing," *SAMPE Journal,* vol. 58, pp. 38-54, 2022.

[7] C. Stokes-Griffin, A. Kollmannsberger, P. Compston and K. Drechsler, "The effect of processing temperature on wedge peel strength of CF/PA6 laminates manufactured in a laser tape placement process," *Composites Part A: Applied Science and Manufacturing,* vol. 121, pp. 84-91, 2019. https://doi.org/10.1016/j.compositesa.2019.02.011.

[8] N. Heathman, P. Koirala, T. Yap, A. Emami and M. Tehrani, "In situ consolidation of carbon fiber PAEK via laser-assisted automated," *Composites Part B, Engineering,* vol. 249, 2023. https://doi.org/10.1016/j.compositesb.2022.110405.

[9] C. Zhang, Y. Duan, H. Xiao, B. Wang, Y. Ming, Y. Zhu and F. Zhang, "The effects of processing parameters on the wedge peel strength of CF/PEEK laminates manufactured using a laser tape placement process," *The International Journal of Advanced Manufacturing Technology volume,* vol. 120, pp. 7251-7262, 2022. https://doi.org/10.1007/s00170-022-09181-5.

[10] A. Kollmannsberger, R. Lichtinger, F. Hohenester, C. Ebel and K. Drechsler, "Numerical analysis of the temperature profile during the laser-assisted automated fiber placement of CFRP tapes with thermoplastic matrix," *Journal of Thermoplastic Composite Materials,* vol. 31, no. 12, pp. 1563-1586, 2018. https://doi.org/10.1177/0892705717738304.

[11] O. Baho, G. Ausias, Y. Grohens and J. Férec, "Simulation of laser heating distribution for a thermoplastic composite: effects of AFP head parameters," *The International Journal of Advanced Manufacturing Technology,* vol. 110, pp. 2105-2117, 2020. https://doi.org/10.1007/s00170-020-05876-9.

[12] C. Stokes-Griffin and P. Compston, "A combined optical-thermal model for near-infrared laser heating of thermoplastic composties in an automated tape placement process," *Composites Part A: Applied Science and Manufacturing,* vol. 75, pp. 104-115, 2014. https://doi.org/10.1016/j.compositesa.2014.08.006.